Supporting Information

In situ preparation of stabilized iron sulfide nanoparticles-impregnated alginate composite for selenite remediation

Jun Wu[1,2], Raymond Jianxiong Zeng[1,2,*]

[1]Fujian Provincial Key Laboratory of Soil Environmental Health and Regulation, College of Resources and Environment, Fujian Agriculture and Forestry University, Fuzhou 350002, China

[2]CAS Key Laboratory for Urban Pollutant Conversion, Department of Chemistry, University of Science & Technology of China, Hefei 230026, PR China

* Correspondence concerning this article should be addressed to:

Raymond J. Zeng at rzeng@ustc.edu.cn. Tel/Fax: +86 591 83303682

This SI contains 24-page document, including 7-page descriptions about chemicals, microorganisms and cultivation, characterization, determination of FeS amount in SA beads, kinetic experiments and isotherm models, effects of pH and anions on the removal efficiency, and column experiment, 5 tables and 11 figures

Chemicals

High-molecular-weight SA (M.W.=200000-270000), $FeSO_4 \cdot 7H_2O$, Na_2SeO_3, ascorbic acid, *o*-phenanthroline, NaCl, Na_2CO_3, Na_3PO_4, $Fe(OH)_3$, $CaCl_2$, HCl, and NaOH were purchased from Sinopharm Chemical Reagent Co., Ltd. (Shanghai, China). $Na_2S \cdot 9H_2O$ was obtained from Aladdin Chemistry Co. Ltd. (Shanghai, China). Iron selenide (FeSe) was purchased from Alfa Aesar (China) Chemical Co., LTD (Shanghai, China). Metal selenium (Se (0)) was purchased from Macklin Biochemical Technology Co., Ltd. (Shanghai, China). 4-(2-hydroxyethyl)-1-Piperazineethanesulfonic acid (HEPES) was from Biosharp Co., Ltd. All solutions were prepared with deionized (DI) water.

Microorganisms and cultivation

SRB, *Desulfovibrio vulgaris* (NBRC 104121), was purchased from National Institute of Technology and Evaluation of Japan. It was first anaerobic cultivated in serum bottle to the stationary phase at 37 ℃ with NBRC medium 1021, which consists of 0.5 g/L K_2HPO_4, 1 g/L NH_4Cl, 1 g/L Na_2SO_4, 0.1 g/L $CaCl_2{\cdot}2H_2O$, 2 g/L $MgSO_4{\cdot}7H_2O$, 2 g/L sodium lactate, 1 g/L yeast extract, 0.5 g/L $FeSO_4{\cdot}7H_2O$, 1 mg/L resazurin, and 10 thioglycolate solution (0.1 g sodium thioglycolate and 0.1 g ascorbic acid were dissolved to 10 mL distilled water, sterilize by filtration). All the chemicals were purchased from Sinopharm Chemical Reagent Co., Ltd. (Shanghai, China).

Characterization

Images obtained by field emission scanning electron microscopy (FE-SEM) were captured on a JEOL JSM-6700F microscope (JEOL, Japan). A thin film of gold was used to increase the conductivity of the samples for SEM. Next, a FeS-SA bead was cut into slices with a microtome Leica CM1950 (Leica, Germany), and the slice was transferred onto the well of a microscope slide before observation. A phase-contrast microscope, Olympus IX81 (Olympus, Japan), was used to observe the gel structure of the slices. Transmission electron microscopy (TEM) was conducted using a JEOL-2010 JSM microscope (JEOL, Japan) at an acceleration voltage of 200 kV. Powder X-ray diffraction (XRD) patterns were recorded at a scanning rate of 0.02°/s in the 2θ range of 10°–60° on a Philips X'Pert ProSuper X-ray diffractometer (Philips, Netherlands) using graphite-monochromatized Cu Kα radiation (λ = 1.54178 Å). Thermogravimetric (TG) analysis was performed with SDT Q600 (TA Instruments, USA) under a stream of air at a heating rate of 10 °C/min. X-ray photoelectron spectroscopy (XPS) was conducted with Thermo Escalab 250 (Thermo VG Scientific, UK) using a monochromatic Al Kα source (1,486.6 eV). The intensity of each XPS peak was recorded in counts per second. A Casa XPS software based on Monte-Carlo method was used to estimate the standard deviation of the component peak areas used in the fitting procedure.

Determination of FeS amount in SA beads

To conduct comparative analysis between FeS-SA beads and pure FeS suspension, the amount of FeS immobilized in alginate beads was measured. Concentrated HCl was diluted with purged DI water to reach 2 M, and then 50 mL of diluted HCl was added to the FeS-SA beads. The solution was taken out to determine the concentration of Fe(II) after 12 h of immersion. The amount of FeS was calculated based on the concentration of Fe(II). Furthermore, due to the stability of FeS-SA after heating at 700 °C,[33] the difference in the weight loss between FeS-SA beads and SA beads was determined by TG analysis, and the amount of FeS was calculated based on the initial weight of FeS-SA. An equal concentration of pure FeS suspension was prepared for a comparison with FeS-SA.

Experiments and isotherm models

Concentrations of 0, 2, 6, 8, 10, 12, 16, and 20 mg/L Se(IV) were set to determine the adsorption isotherm, and the Se(IV) concentration and final pH were measured after equilibrium. Freundlich and Langmuir models adsorption isotherms were utilized to describe the adsorption equilibrium.

Langmuir isotherm model is represented mathematically as bellows:

$$q_e = \frac{q_m K_L C_e}{1 + K_L C_e}$$

In this equation q_e is the equilibrium adsorption quantity (mg/g), C_e is the equilibrium liquid phase concentration (mg/L), q_m is the maximum adsorption capacity (mg/g). The Freundlich model can be represented as bellows:

$$q_e = K_F C_e^{1/n}$$

q_e is the equilibrium adsorption quantity (mg/g), C_e is the equilibrium liquid phase concentration (mg/L), K_F and n denoting a distribution coefficient ((mg/g)/(mg/L)^n) and intensity of adsorption, respectively.

Effects of pH and anions on the removal efficiency

Batch equilibrium tests were conducted in 50-mL glass vials to investigate the effects of pH and anions (e.g., NaCl, Na_2CO_3, and Na_3PO_4) on Se(IV) removal efficiency using FeS-SA beads. Each vial was loaded with Se(IV) at a concentration of 10 mg/L. The initial pH of the mixture was adjusted within the range from 4 to 10. The concentrations of anions were set between 0 and 120 mg/L. The solutions were placed in a shaker (at 170 rpm) at room temperature (25 °C) to reach equilibrium and were then sampled to measure the concentration of Se(IV).

Column experiment

Dynamic flow adsorption experiments were performed in a glass column with an internal diameter of 1.2 cm and a length of 30 cm to evaluate the breakthrough behavior and the applicability of FeS-SA for the removal of Se(IV) under dynamic conditions. The column was packed with FeS-SA beads and shaken so that higher amounts of FeS-SA beads were packed in the column without gaps. The influent solution was pumped into the column by a Longer Pump (BT100-1L) at a flow rate of 10 mL/h in an up-flow mode, ensuring that more contact time was obtained and any channeling of the influent solution reduced. The influent concentration was maintained at 10 mg/L. The effluent solution was collected at different time intervals, and the concentration of Se(IV) was monitored. The adsorption bed was considered to be exhausted when the effluent concentration reached 10 mg/L.

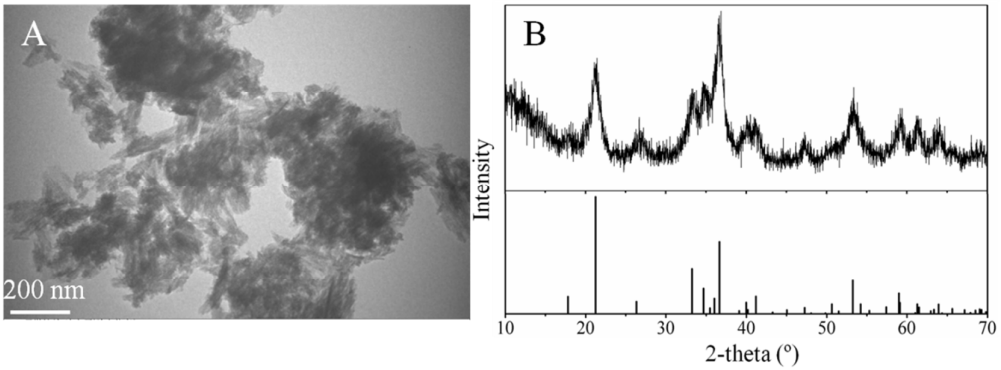

101

102 **Figure S1.** (A) TEM and (B) XRD patterns of the α-FeOOH; (Goethite, JCPDS:

103 81-0464).

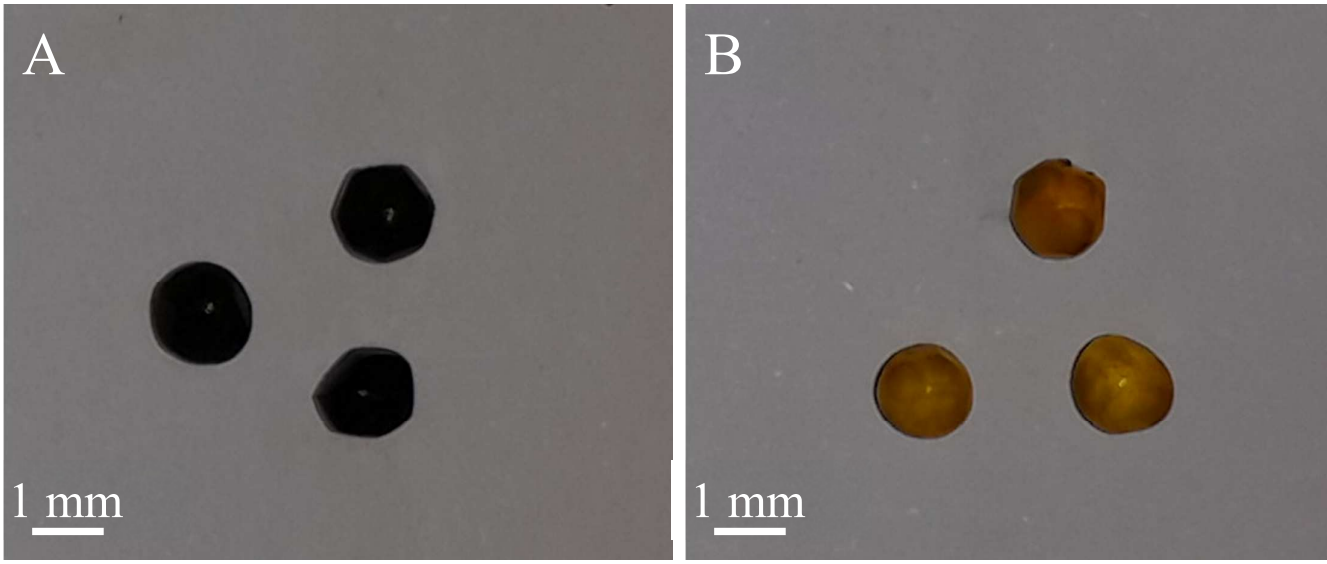

Figure S2. Photograph of FeS-SA (A) before and (B) after reacting with Se(IV).

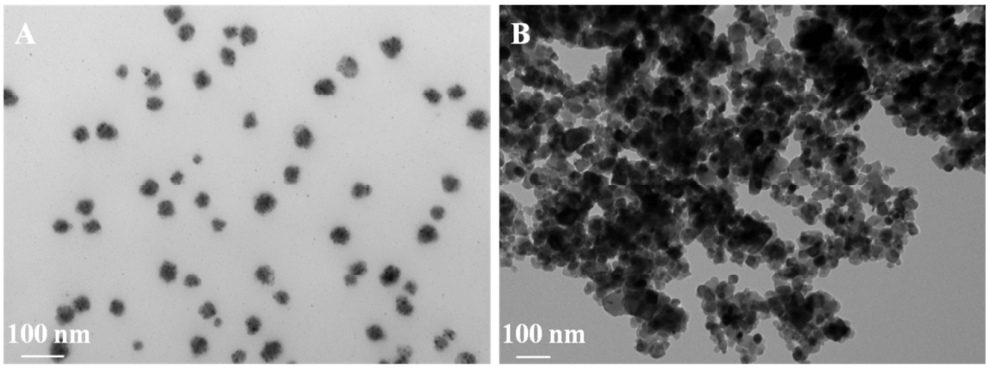

106

107 **Figure S3.** TEM of (A) FeS nanoparticles stabilized by SA (B) non-stabilized FeS.

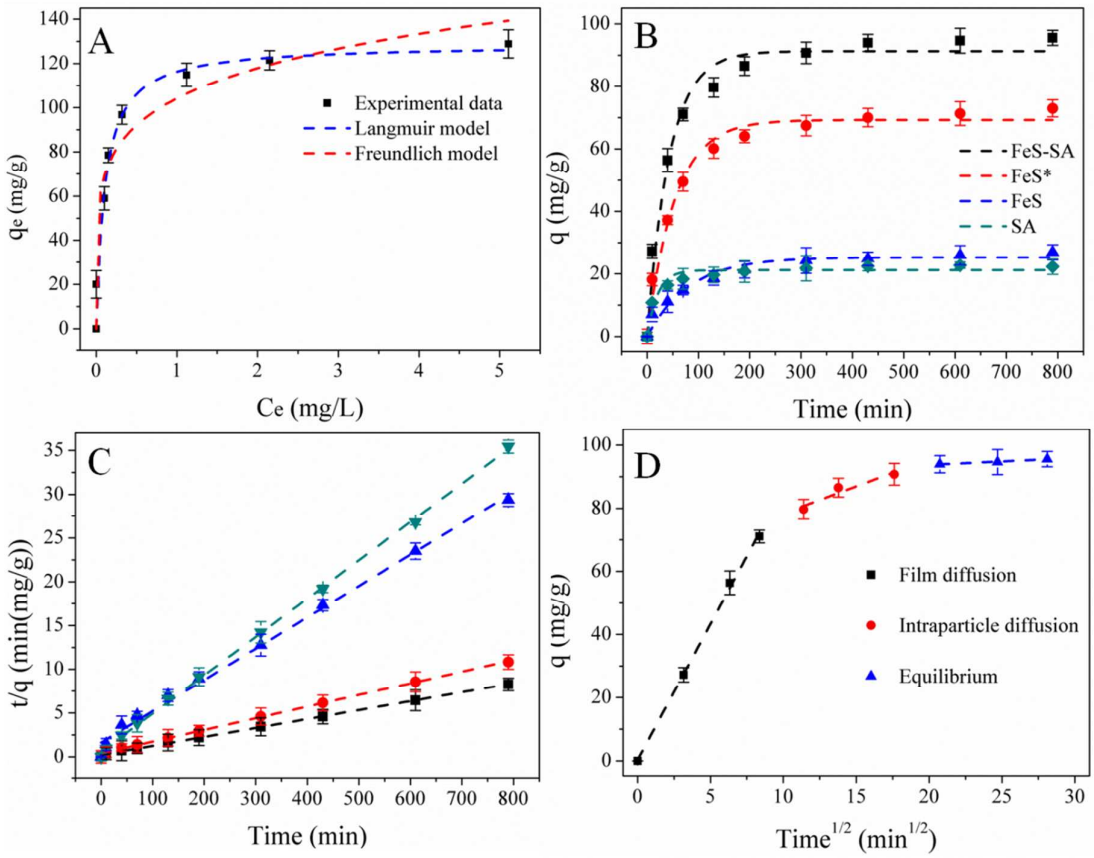

Figure S4. (A) Se(IV) removal isotherm of FeS-SA beads. Initial Se = 2−20 mg/L, initial pH = 6.0 ± 0.1. Se(IV) removal kinetics of (B) pseudo-first-order, (C) pseudo-second-order, and (D) Weber-Morris fittings by FeS-SA. Initial Se = 10 mg/L, initial pH = 6.0 ± 0.1. Symbols: experimental data; lines: model fittings.

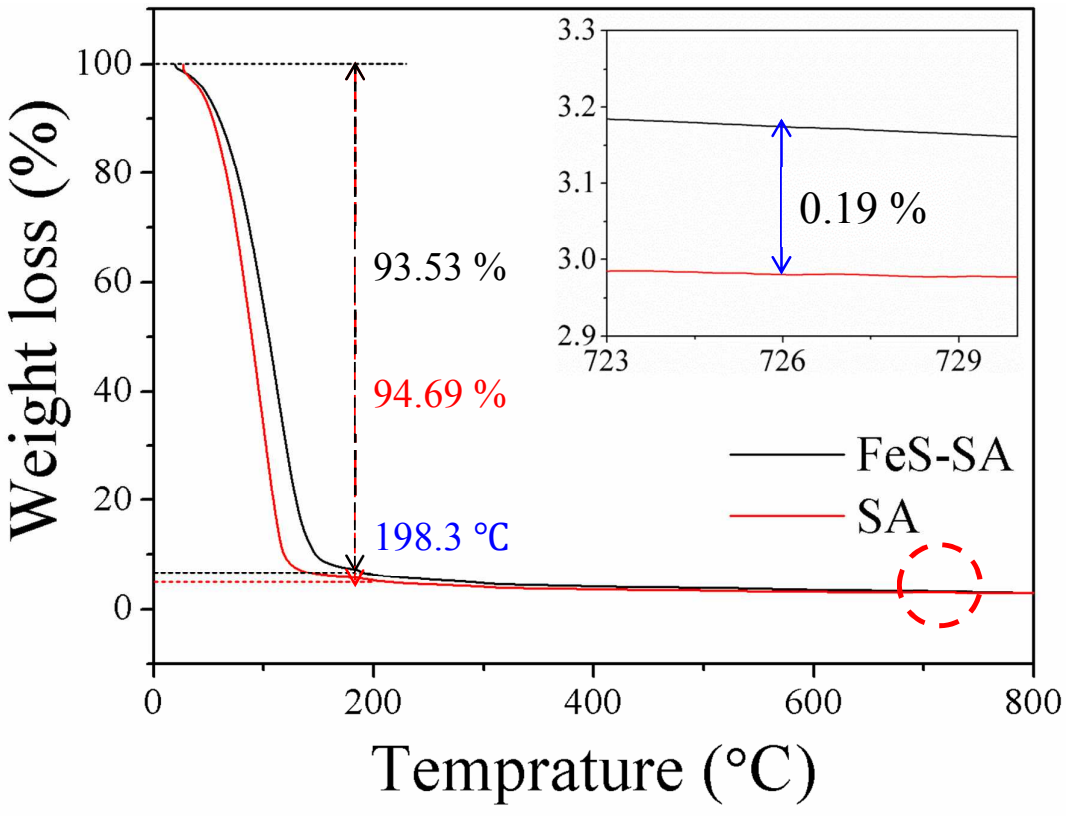

Figure S5. TG curve of FeS-SA and SA.

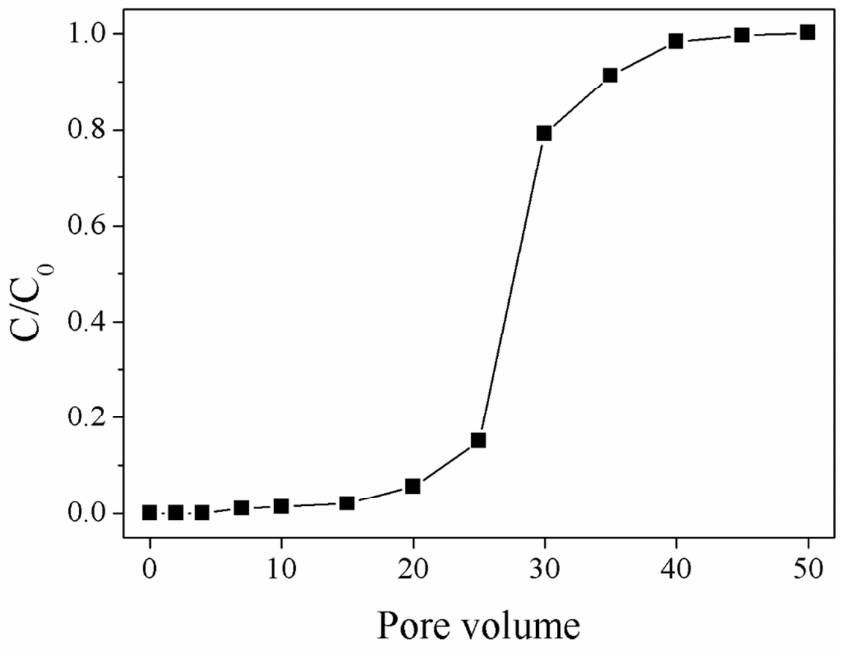

114

115 **Figure S6.** Breakthrough curves of Se(IV) through fixed-bed column containing

116 FeS-SA. Influent Se(IV) = 10 mg/L, flow rate =10 mL/h, pH = 6.0 ± 0.2.

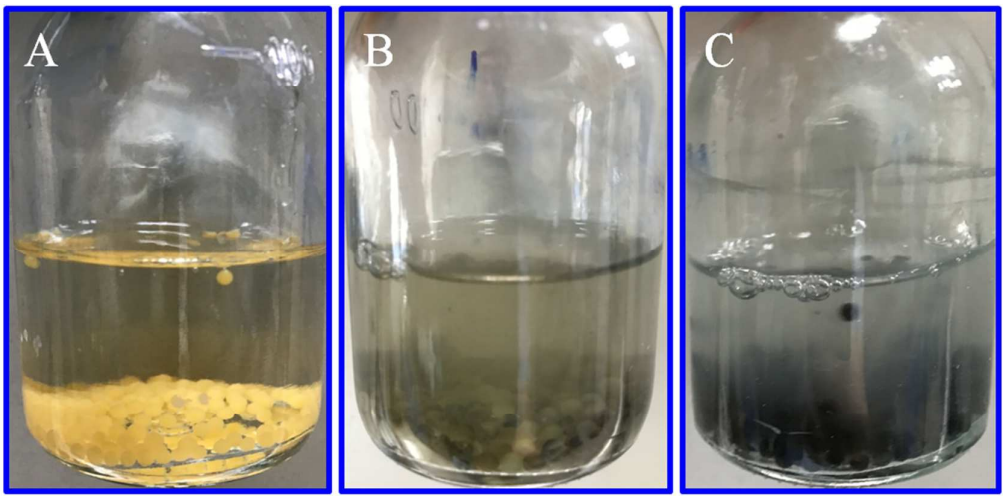

Figure S7. Photograph of the process of FeS-SA regeneration at (A) 0 h, (B) 12 h, and (C) 24 h in the presence of SRB.

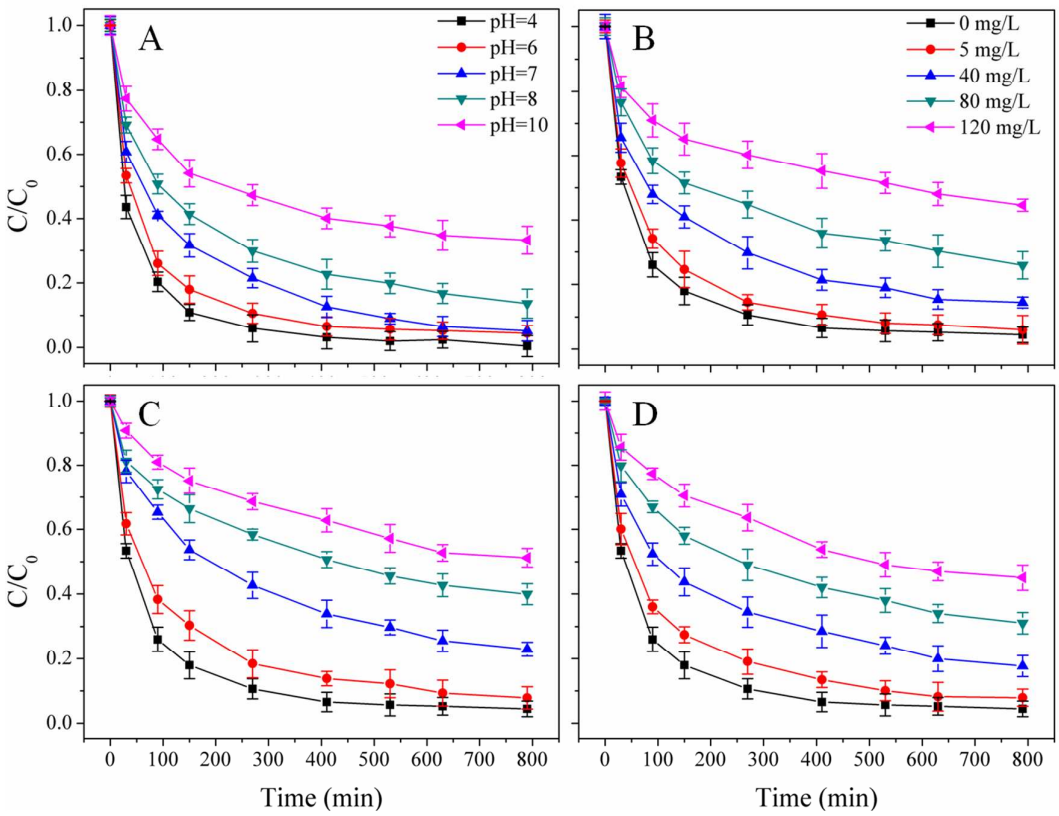

Figure S8. The effects of (A) pH, initial Se = 10 mg/L, and different concentration (B) phosphate, (C) carbonate, and (D) chloride on the reactivity of FeS-SA for the removal of Se(IV); initial Se = 10 mg/L, initial pH = 6.0 ± 0.2 (Errors given as standard deviation among triplicate samples).

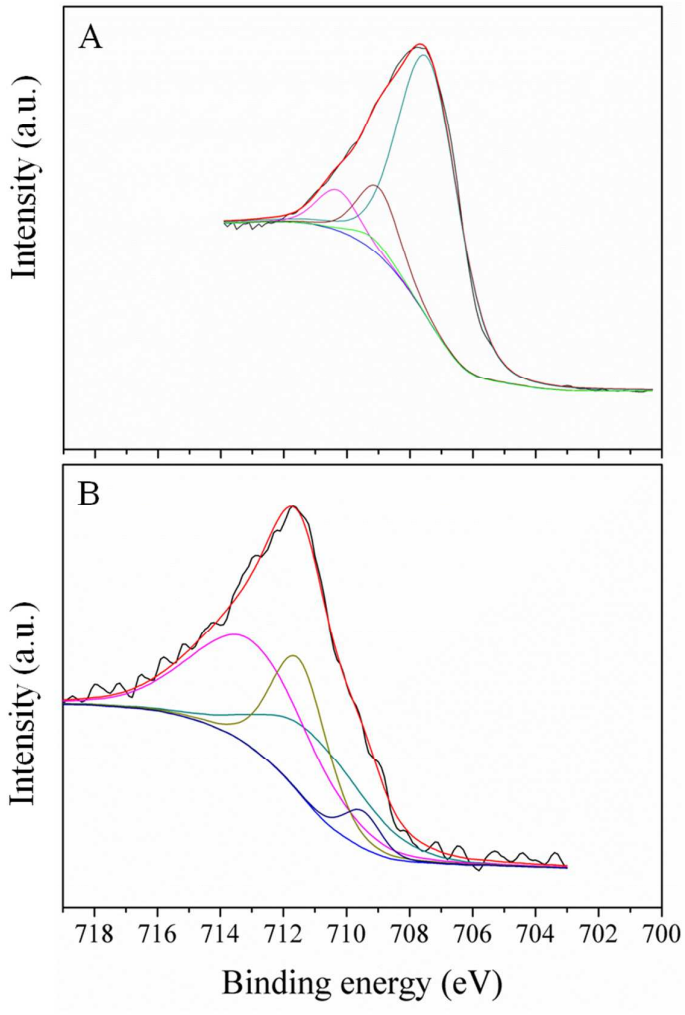

125

126 **Figure S9.** Fe 2p3/2 XPS spectra of FeS-SA bead (A) before (B) after Se(IV) removal

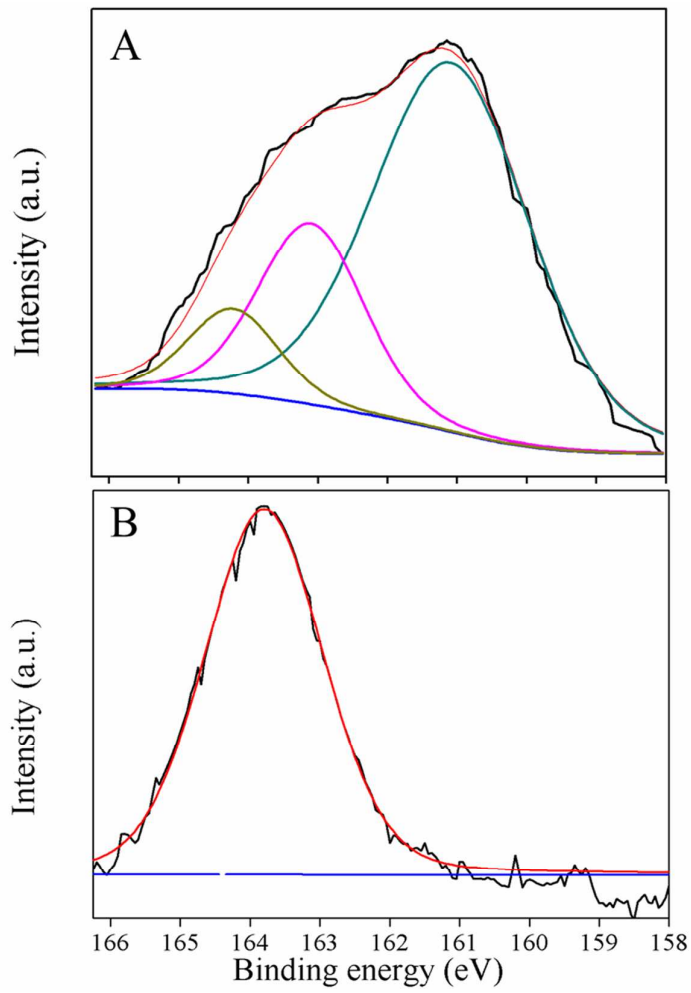

127

128 **Figure S10.** S 2p3/2 XPS spectra of FeS-SA bead (A) before (B) after Se(IV) removal

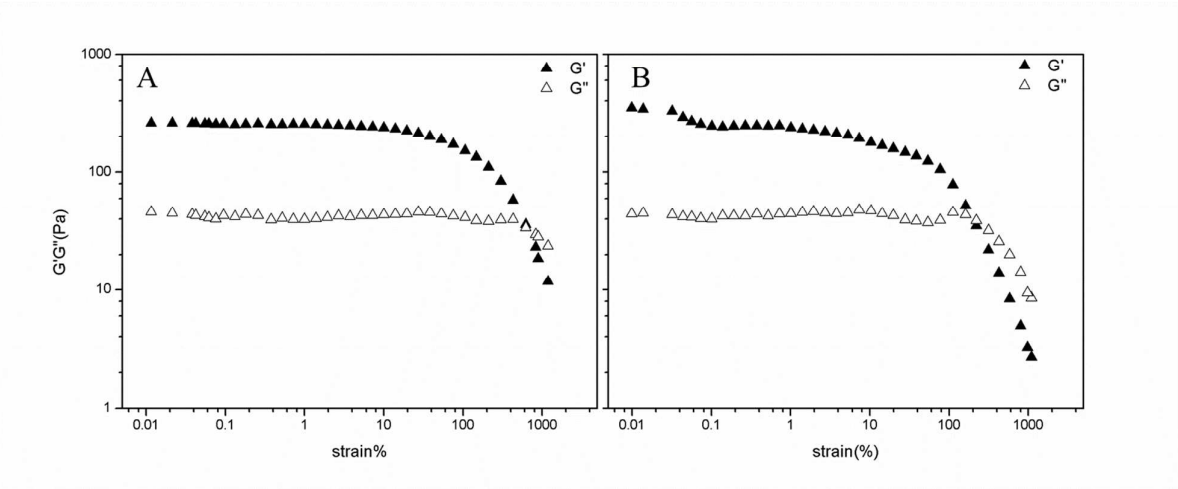

129 **Figure S11**. Strength analysis of FeS-SA beads (A) before (B) after Se(IV) treatment.

130 **Table S1.** Best-fitted parameters for Langmuir and Freundlich isotherm models

131 (Errors given as standard deviation among triplicate)

Adsorption isotherm	Parameters		R^2
Langmuir	q_m (mg/g)	K_L(L/mg)	
	128.7 ± 5.6	9.4 ± 2.0	0.972
Freundlich	K_F, (mg/g)/(mg/L)^n	n	
	104.2 ± 4.0	5.6 ± 0.8	0.960

Table S2. Se(IV) removal efficiency in various species and separated component

Species	Removal efficiency (%)	Separated component removal efficiency (%)			
		SA	FeS	α-FeOOH	Stabilized effect
FeS	27	0	27	0	0
FeS*	73	0	27	0	46
SA	20	20	0	0	0
FeS-SA	100	20	27	0	46
FeS-SA*	40	20	0	11	9
α-FeOOH-SA	31	20	0	11	0

Table S3. Pseudo-first-order and pseudo-second-order models used for simulating Se(IV) removal kinetic data and the resulting fitting parameters (Errors given as standard deviation)

Kinetic models		Parameters		R^2
		q_e (mg/g)	K_1(min^{-1})	
Pseudo-first-order	FeS-SA	91.3 ± 2.1	(2.3 ± 0.3) ×10^{-2}	0.979
	FeS*	69.3 ± 1.5	(1.9 ± 0.2) ×10^{-2}	0.984
	FeS	25.3 ± 0.9	(1.2 ± 0.2) ×10^{-2}	0.959
	SA	21.2 ± 0.7	(4.5 ± 1.0) ×10^{-2}	0.945
		q_e (mg/g)	K_2(g/(mg·min))	
Pseudo-second-order	FeS-SA	98.0 ± 1.3	(4.5 ± 0.8) ×10^{-4}	0.999
	FeS*	75.0 ± 1.1	(4.6 ± 0.8) ×10^{-4}	0.998
	FeS	27.9 ± 0.7	(7.9 ± 1.7)×10^{-4}	0.994
	SA	22.8 ± 0.2	(33.8 ± 7.6)×10^{-4}	0.999

Pseudo-first-order model is represented as：

$$q = q_e(1 - e^{-K_1 t})$$

Pseudo-second-order model is described as:

$$\frac{t}{q} = \frac{1}{K_2 q_e^2} + \frac{1}{q_e} t$$

In the equation qe is the equilibrium adsorption quantity (mg/g), q is the adsorption capacity (mg/g), K_1 is pseudo-first-order rate constant (min^{-1}), K_2 is pseudo-second-order rate constant (g/(mg·min)

Table S4. Best-fitted parameters for Weber-Morris model for Se(IV) removal kinetic data.

Diffusion models	stages	Parameters		
		K_w	C	R^2
Weber-Morris	Film diffusion	8.6 ± 0.2	0.3 ± 0.1	0.998
	Intraparticle diffusion	1.7 ± 0.5	61.2 ± 6.9	0.890
	Equilibrium	0.2 ± 0.03	89.4 ± 0.7	0.962

In Weber-Morris model, Curves are commonly interpreted as a three-stage linear plot with an external mass transfer-controlled phase, an intraparticle mass transfer-controlled phase, and the equilibrium phase. If plotting q, below equation vs. $\sqrt{t}$ yields a linear relation through the origin, this is seen as evidence for mass transfer control.[36] Following equations will be defined assuming that all particles are uniform spheres of radius R.

$$q=K_w\sqrt{t}+C$$

where q is adsorption capacity at time t, and q_e is equilibrium adsorption quantity after an infinite time, K_w is intraparticle diffusion rate constant, C is related to thickness of beads.

Table S5. XPS analytic results based on the curve fitting for Fe 2p3/2 and S 2p3/2 peaks before and after reaction in Figures S9 and S10.

Element		Binding energy (eV)	Species	Relative fraction (%)
Fe(2p3/2)	Before	707.4	Fe (II)-S	79.6 ± 2.3
		709.0	Fe(II)-O	6.4 ± 0.6
		709.3	Fe (III)-S	3.4 ± 1.6
		710.3	Fe (II)-S	10.6 ± 2.1
	After	710.9	FeSe	26.8 ± 3.6
		711.5	α-FeOOH	25.9 ± 2.8
		709.3	Fe (II)-O	4.3 ± 1.1
		713.0	Fe (III)-O	43.0 ± 1.7
S(2p3/2)	Before	161.3	S(-II)	71.3 ± 2.7
		163.4	S_n(-II)	25.6 ± 1.3
		164.0	S_n(0)	3.1 ± 0.4
	After	164.0	S_n(0)	100 ±1.2